PERGAMON

International Journal of Heat and Mass Transfer 43 (2000) 241–250

International Journal of HEAT and MASS TRANSFER

www.elsevier.com/locate/ijhmt

A dry-spot model of critical heat flux applicable to both pool boiling and subcooled forced convection boiling

Sang Jun Ha[a,*], Hee Cheon No[b]

[a]Nuclear Power Laboratory, Korea Electric Power Research Institute, 103-16 Munji-Dong Yusong-gu, Taejon 305-380, South Korea
[b]Department of Nuclear Engineering, Korea Advanced Institute of Science and Technology, 373-1 Kusong-dong Yusong-gu, Taejon 305-701, South Korea

Received 9 April 1999

Abstract

A phenomenological model of critical heat flux (CHF) applicable to both pool boiling and subcooled forced convection boiling is developed using the dry-spot model proposed recently and existing correlations for active site density, bubble departure diameter and heat transfer coefficient in nucleate boiling. For the active nucleation site density Kocamustafaogullari and Ishii's model is used including the concept of a suppression factor. The Chen correlation is used for the estimation of total heat flux in nucleate boiling. Comparisons of the model predictions with experimental data for pool boiling of water and subcooled upward flow boiling of water in vertical, uniformly-heated round tubes yield an averaged CHF ratio of 0.93 and a root-mean-square error of 41.3%. The data set compared for CHF in subcooled forced convection boiling covers wide ranges of operating conditions ($0.1 \leqslant P \leqslant 14.0$ MPa, $0.00033 \leqslant D \leqslant 0.0375$ m; $0.002 \leqslant L \leqslant 2$ m; $660 \leqslant G \leqslant 90{,}000$ kg/m^2 s; $70 \leqslant \Delta h_i \leqslant 1456$ kJ/kg). By the modification of the suppression factor only the predictive capability of the present model is greatly improved with a r.m.s. error of 20.5%.

1. Introduction

The accurate prediction of CHF in pool and forced convection boiling is of importance in a wide variety of process equipment. A great volume of experimental and analytical studies on the CHF have been conducted by many researchers during the last several decades. State-of-the-art overview of the phenomena and prediction models and correlations are available in the literature [1,2]. Generally, the CHF under forced convective conditions is classified into two groups: departure from nucleate boiling (DNB) at subcooled or low-quality regions and liquid film dryout (LFD) at high quality. The physical mechanism of the LFD is relatively well understood. However, the detailed aspects of the DNB mechanism have not been clearly understood [3–6].

Extensive research efforts have been devoted to the modeling of the DNB. However, due to the difficulty in performing detailed visualization of the phenomena occurring at the interface between fluid and heating surface, most of the published models have been based on postulated mechanisms. Generally, the major theoretical approaches to DNB can be classified into five groups according to the basic mechanism postulated as the main cause of the CHF occurrence: liquid layer superheat limit model [7], boundary layer separation model [8], liquid flow blockage model [9], vapor removal limit and near-wall bubble crowding model

* Corresponding author. Tel.: +82-42-865-5678; fax: +82-42-865-5504.
E-mail address: hsj@kepri.re.kr (S.J. Ha)

0017-9310/00/$ - see front matter
PII: S0017-9310(99)00135-0

Nomenclature

A	cell area [m^2]
CHFR	predicted to measured CHF ratio
c_p	specific heat [J/kg K]
D	tube diameter [m]
d	bubble diameter [m]
d_{av}	time-averaged bubble diameter [m]
d_{max}	bubble diameter at departure [m]
F	parameter
G	mass flux [kg/m^2 s]
g	gravitational acceleration [$kg/m\ s^2$]
h	heat transfer coefficient [W/m^2 K]
h_c	convective heat transfer coefficient [W/m^2 K]
h_{fg}	latent heat of vaporization [J/kg]
h_{NB}	nucleate boiling heat transfer coefficient [W/m^2 K]
Δh_i	inlet subcooling enthalpy [kJ/kg]
k	thermal conductivity [W/m K]
L	tube length [m]
N	average density of active sites [$sites/m^2$]
n	number of active nucleation sites
n_c	critical active site number
P	probability function defined by Eq. (3) or pressure [N/m^2]
Pr	Prandtl number
q	heat flux [W/m^2]
q_b	heat transferred by single bubble site [W/site]
q_{nb}	heat flux fitting the nucleate boiling data [W/m^2]
Re_{TP}	two-phase Reynolds number
R_g	ideal gas constant [J/kg K]
S	suppression factor defined by Eq. (11)
T	temperature [K]
ΔT	wall superheat [K]
ΔT_e	effective wall superheat [K]
t	time [s]
X	quality
X_{tt}	Martinelli parameter
z	axial coordinate [m]

Greek symbols

μ	viscosity [$N\ s/m^2$]
ρ	density [kg/m^3]
σ	surface tension [N/m]
ϕ	contact angle [deg]

Subscripts

f	liquid phase
g	gas phase
sat	saturation condition
sub	subcooled condition
w	wall

Superscript

$'$	dimensionless quantities

[10,11], and liquid sublayer dryout model [12–14]. A detailed discussion of the above models has been given in Refs. [3–5]. Currently, among the models mentioned above, only the bubble crowding model and the liquid sublayer dryout model are receiving significant attention. According to Chang and Baek [6], Weisman and Pei model [10] shows good prediction for the high pressure region relevant to pressurized water reactor conditions, while the Katto model [13] or Celata et al. model [14] for low-pressure, high-flow conditions relevant to fusion applications.

In spite of good agreement of the models and experimental data within the applicable ranges of each model, there are some reasons which make one to doubt the validity of the physical features of the models. Bricard and Souyri [5] have critically reviewed existing DNB models by taking into account the experimental observations published in the literature. And they concluded that the mechanisms postulated by Weisman and Pei [10], Lee and Mudawar [12] and Katto [13] are not precisely related to experimental observations and that the basic mechanism of DNB is tightly linked to the phenomena of bubble nucleation based on the following facts: no change of flow structure at DNB encountered in bubbly and slug flow, the coalescence of bubbles and an appearance of intermittent local vapor film in bubbly flow, and the nucleation of bubbles and their coalescence in the sublayer in slug flow.

The other problem involved in many existing DNB models is that most of the models make use of empirical constants or tuning factors deduced from a best-fit procedure through available CHF data sets. The empirical constants or tuning factors tend to cloud the mechanism of CHF. Therefore, to develop a model without any tuning factors is very important to clarify the fundamental understanding of the process. Celata et al. [14] tried to eliminate all the empiricisms through rationalization of liquid sublayer dryout model proposed by Lee and Mudawar [12] and Katto [15]. The liquid sublayer dryout model is based on the macrolayer dryout model [16] postulating the onset of CHF

due to the dryout of a thin liquid layer (macrolayer) underneath a vapor blanket. However, the macrolayer dryout model has some problems on the physical features of the model as pointed out by Ha and No [17]

In addition, most of the DNB models assume specific CHF mechanisms for specific ranges of parameters in subcooled forced convection boiling. However, the form of the CHF variations as a function of local quality does not change when the local quality changes as noted by Bricard and Souyri [5]. It may support that the CHF mechanism would be the same in subcooled forced convection boiling. Del Valle and Kenning [18] observed that the change of flow regime from bubbly to slug flow before CHF does not affect the shape of the boiling curve.

The boiling phenomena in subcooled forced convection boiling are quite similar to those in pool boiling in the view of the following facts: (1) the distribution of active site density and an increase in active site density as wall superheat increases; (2) the coalescences of bubbles and formation of dry area in nucleate boiling; (3) no change of bulk flow pattern at CHF; and (4) the CHF is affected by the influences of fluid side as well as by the influences of heater side.

Summarizing the facts discussed above, the CHF may be related to certain phenomena at very near-wall region and may be linked to the phenomena of nucleation of bubbles and their coalescences. Also, the similarity in boiling phenomena between pool boiling and subcooled flow boiling may support that the basic CHF mechanism of subcooled flow boiling is also similar to CHF in pool boiling.

From these view points, a phenomenological dry-spot model has been developed for CHF. prediction in pool boiling and subcooled forced convection boiling by the authors [17,19]. The model has been based on the mechanism that CHF is caused by the accumulation and coalescences of dry spots formed through dryout of the microlayer under a bubble. One of important features of this model is that CHF is considered as an process not independent of nucleate boiling but its extension. In other words, if information on boiling parameters such as active site density and bubble departure diameter, etc. in nucleate boiling is known, CHF can be determined from the extension of this information as a function of wall superheat.

The aim of the present paper is to develop a CHF model in pool boiling and subcooled forced convection boiling using the dry-spot model and existing correlations for boiling parameters in nucleate boiling. Due to our limited understanding on active site density and bubble diameter for given boiling conditions [20], in the present study, emphasis will be placed on the fundamental understanding of the CHF mechanism and finding a CHF model applicable over wider operation conditions without tuning factors rather than the prediction accuracy of the present model. By assuming that the applicable ranges of each correlation for boiling parameters can be extended to the range of the CHF data selected in the present study, the CHF predictions from the model will be compared with data in saturated water pool boiling and subcooled upward flow boiling of water in vertical, uniformly-heated round tubes. Also the parametric trends of CHF in subcooled forced convection boiling will also be investigated.

2. The dry-spot model

The dry-spot model is based on the boiling phenomena in nucleate boiling such as Poisson distribution of active nucleation sites and formation of dry spots on the heating surface. It is hypothesized that when the number of bubbles surrounding one bubble exceeds a critical number, the surrounding bubbles restrict the feed of liquid to the microlayer under the bubble. Then an insulating dry spot of vapor will form on the heated surface. The CHF is caused by the accumulation and coalescences of the dry spots. The basic mechanism of the CHF is the same in both pool boiling and subcooled forced convection boiling.

The overall heat flux is expressed by the following equation:

$$q = q_b \bar{N}(1 - P(n \geq n_c)), \tag{1}$$

where

$$P(n \geq n_c) = 1 - \sum_{n=0}^{n_c-1} P(n), \tag{2}$$

$$P(n) = \frac{e^{-\bar{N}A}(\bar{N}A)^n}{n!}, \tag{3}$$

q_b is heat transferred by a single bubble site, $\bar{N}$ is active site density, and n_c is a critical site number to form the dry spot under a bubble and determined by 5 in Ref. [17]. A is cell area. The diameter of the cell is taken as twice that of the bubble, i.e. $A = \pi d_{av}^2$. Time-averaged bubble diameter d_{av} is representative of the diameter of bubbles for coexisting bubbles of all ages. The physical meaning of notations used in above equations are described in detail in Ref. [17]. In water pool boiling and subcooled forced convection boiling, the calculation of the quantities, $\bar{N}$, d_{av} and q_b, in the above equations will be presented in the following section.

3. Existing correlations for boiling parameters in nucleate boiling

3.1. Pool boiling

The active nucleation site density $\bar{N}$ is obtained from the pool boiling correlation developed by Kocamustafaogullari and Ishii [21]. The correlation is expressed as

$$\bar{N}' = f(\rho')R_c'^{-4.4}, \tag{4}$$

where the dimensionless nucleation site density, $\bar{N}'$, the dimensionless cavity size, R_c', and the pressure dependent function, $f(\rho')$, are defined as

$$\bar{N}' = \bar{N}d_{max}^2; \quad R_c' = 2R_c/d_{max}, \tag{5}$$

$$f(\rho') = 2.157 \times 10^{-7}\rho'^{-3.2}(1 + 0.0049\rho')^{4.13}, \tag{6}$$

where $\rho' = (\rho_f - \rho_g)/\rho_g$, and the cavity radius, R_c, and the bubble departure diameter, d_{max}, are expressed as

$$d_{max} = 0.0012(\rho')^{0.9}d_F, \tag{7}$$

$$R_c = \frac{2\sigma}{P_f}(1 + \rho_g/\rho_f)(\exp[h_{fg}(T_g - T_{sat})/R_gT_gT_{sat})/R_gT_gT_{sat}] - 1)^{-1}. \tag{8}$$

In Eq. (7), d_F is the bubble departure diameter of Fritz given as $d_F = 0.0208\phi(\sigma/g\Delta\rho)^{1/2}$. For the pool boiling $T_g - T_{sat} \cong \Delta T_{sat}$ is used [21]. The correlation for bubble departure diameter, Eq. (7), is applicable for water over a pressure range of 0.1–14.1 MPa [22]. The contact angle ϕ in Fritz's equation represents the characteristic of the combination of liquid and surface. Active nucleation site density $\bar{N}$ is predicted using Eqs. (4)–(8). Time-averaged bubble diameter d_{av} is calculated from Eq. (7) assuming that the bubble diameter varies with times as $t^{1/2}$ [23], i.e. $d_{av} = 2/3d_{max}$.

To obtain the heat transfer q_b in Eq. (1), the following heat transfer correlation proposed by Kocamustafaogullari and Ishii [21] is used:

$$h = 14.0(k_f\bar{N}^{0.5})[(\rho_f c_{pf}\Delta T_{sat})/\rho_g h_{fg}]^{0.5}Pr_f^{0.39}\bar{N}'^{-0.125}. \tag{9}$$

Assuming that if there is no generation of dry spots on the heating surface, heat flux will increase along the extension of nucleate boiling and that each bubble site has uniform heat duty, q_b can be evaluated from the following equation:

$$q_b = \frac{h\Delta T_{sat}}{\bar{N}}. \tag{10}$$

3.2. Subcooled forced convection boiling

In the case of subcooled forced convection boiling, there are very few experimental data providing quantitative information on active nucleation site density. Based on the concepts of the mechanistic similarity in bubble nucleation between pool boiling and convective nucleate boiling, Kocamustafaogullari and Ishii [21] postulated that the active nucleation site density correlation developed for pool boiling, Eq. (4), could be used in forced convective boiling by using effective superheat ΔT_e rather than actual wall superheat ΔT_{sat} because the temperature gradient through a liquid film in which bubbles grow is affected by the hydrodynamic flow field. To evaluate the vapor temperature T_g in Eq. (8), they introduced the concept of a suppression factor S proposed by Chen [24]:

$$S = (\Delta T_e/\Delta T_{sat})^{0.99}, \tag{11}$$

where $\Delta T_e = T_g - T_{sat}$. S can be calculated from fitting Chen's representation for S

$$S = 1/(1 + 1.5 \times 10^{-5}Re_{TP}), \tag{12}$$

where Re_{TP} is two-phase flow Reynolds number defined by

$$Re_{TP} = [G(1 - X)D/\mu_f]F^{1.25}, \tag{13}$$

where

$$F = 1.0 \quad \text{for} \quad X_{tt} \geq 10,$$

$$F = 2.35(0.213 + 1/X_{tt})^{0.736} \quad \text{for} \quad X_{tt} < 10. \tag{14}$$

For simplicity the power 0.99 in Eq. (11) is replaced by 1.0 and the effective superheat is calculated by

$$\Delta T_e = S\Delta T_{sat}. \tag{15}$$

Chen's heat transfer correlation has been proved to be reliable in subcooled and saturated nucleate boiling [1]. For the subcooled boiling, the total heat flux in nucleate boiling, q_{nb}, can be represented by the following equation:

$$q_{nb} = h_{NB}(T_w - T_{sat}) + h_c(T_w - T_f(z)), \tag{16}$$

where

$$h_{NB} = 0.00122\left(\frac{k_f^{0.79}c_{pf}^{0.45}\rho_f^{0.49}}{\sigma^{0.5}\mu_f^{0.29}H_{fg}^{0.24}\rho_g^{0.24}}\right)\Delta T_{sat}^{0.24}\Delta P_{sat}^{0.75}S, \tag{17}$$

$$h_c = 0.023(G(1 - X)D/\mu_f)^{0.8}(\mu c_p/k)_f^{0.4}(k_f/D)(F). \tag{18}$$

S and F are given by Eqs. (12) and (14), respectively,

and X_{tt} is the Martinelli parameter [1]. According to Collier and Thome [1], for subcooled boiling, the nucleate boiling coefficient h_{NB} is evaluated from Eq. (17) with the value of S obtained from the single-phase liquid Reynolds number and the convective heat transfer coefficient h_c is obtained from Eq. (18) with F set equal to unity. Since the suppression factor and in turn the effective superheat at given wall superheat decreases with increasing mass flux or decreasing quality, the active site density decreases with increasing mass flux or decreasing quality. Based on the CHF mechanism proposed in the present model, when the active site density decreases at given wall superheat, a further increase in wall superheat is needed to reach a critical heat flux conditions. Therefore, it is expected that CHF will increase with increasing mass flux or decreasing quality. The heat transfer q_b for convective boiling can be obtained by substituting Eq. (14) into Eq. (10) with $h\Delta T_{sat}$ replaced by q_{nb}.

3.3. CHF prediction procedure

The basic CHF calculation procedures using Eqs. (1)–(3) are the same for pool boiling and subcooled forced convection boiling. In the case of pool boiling, since the correlations for active site density and heat transfer coefficient are given as a function of wall superheat explicitly, the boiling curve showing the dependence of the heat flux on wall superheat is plotted by substituting Eqs. (4)–(10) into Eqs. (1)–(3). The maximum value of heat flux is taken as the predicted CHF. The calculation procedure for subcooled forced convection boiling depends on the form of given CHF data set. Generally, the CHF data is given in two different forms: the inlet conditions form and the local conditions form. For the case of inlet conditions form, the CHF data are given for fixed system pressure (P), mass flux (G), tube length (L), tube diameter (D) and inlet subcooling (Δh_i). For the case of local conditions form, the CHF data are given for fixed P, G, D and local quality (X) assuming that the tube length has a small effect on the CHF.

For the data given by inlet conditions form, to predict the CHF at a known P, G, L, D, and Δh_i, the steps are as follows:

1.1. Calculate necessary physical properties and d_{av} at saturation pressure.

1.2. Set a value of heat flux q_{nb} in Eq. (16) as a known value. In the beginning, q_{nb} should be larger than the heat flux at which the heater surface temperature lies above the saturation temperature.

1.3. As the critical condition of subcooled forced convection boiling of uniformly-heated round tubes generally occurs at a point near the tube exit, calculate liquid bulk temperature at the exit of the tube by the following heat balance equation:

$$T_f(L) = T_{sat} + \frac{1}{c_{pf}}\left[\frac{4q_{nb}L}{GD} - \Delta h_i\right]. \tag{19}$$

1.4. Calculate wall temperature using the Chen correlation, Eq. (16).

1.5. Calculate q_b and $\bar{N}$ for the calculated wall temperature, and in turn $P(n \geqslant n_c)$ by Eq. (2) using $\bar{N}$ and d_{av}.

1.6. If $\bar{N}$ decreases with an increase in wall superheat or the wall temperature is larger than the critical temperature, CHF cannot be predicted by the present model. Even though the present analysis is limited to subcooled boiling ($X < 0$), the quality corresponding to q_{nb} may be larger than zero in case of overestimation of CHF from the present model. In this case, active site density can decrease as wall superheat increases when the influence of quality is more dominant than that of wall superheat on effective wall superheat in Eq. (15).

1.7. Calculate heat flux q using Eq. (1).

1.8. If the CHF condition is not reached, increase heat flux q_{nb} and iterate steps 1.3.–1.7.

For the data given by local conditions form, although the overall procedure is similar to the above one, an iteration procedure to meet given local quality is needed. The calculation procedure is as follows:

2.1. Put a value of L as a known value and assume Δh_i.

2.2. Calculate heat flux by the present model and quality at the exit (X_p) and check whether the condition of CHF is reached or not through steps 1.1.–1.8.

2.3. When $X_p = X$, the calculated heat flux is the critical heat flux.

2.4. If $X_p \neq X$, adjust Δh_i and iterate steps 2.1.–2.3. until $X_p = X$.

4. Results and discussion

The applicable ranges of the correlations used in the present study are summarized in Table 1. During the selection of experimental CHF data for comparison with predictions from the present model, only the pressure range of the CHF data is limited within a valid range of the correlation for bubble departure diameter. As for the ranges of other independent variables of the CHF data, it is assumed that the applicable ranges of each correlation can be extended to the range of data selected.

4.1. Comparison with CHF data in pool boiling

The predictions from the present model are compared with the water data from Kazakova [25]. The data at CHF were obtained by Kazakova with a

Table 1
Range of conditions for correlations used in the present study

Correlation	Flow mode	P (MPa)	G (kg/m^2 s)	ΔT_{sub} (K)	q (MW/m^2)	Heater geometry
Bubble departure diameter [22]	pool	0.1–14.1		saturation		
	flow			subcooled (12 K)		
Active nucleation site density [21]	pool	0.1–19.8		saturation		
	flow	0.5–5.0	457–1720	13–85	0.4–5.0	plate
Chen correlation [24]	flow	0.06–3.4	54–4070	saturation (X = 0–0.7)	0–2.4	tube annulus

10 mm diameter disk heater with contaminated surface. As for the contact angle, Hsu and Graham [26] reported that contact angles between most industrial metals and water lie within 40–60°. Fig. 1 shows the comparison of the predictions with the experimental data for various contact angles. The model predictions for contact angle 45° show the best agreement with the data. Although the contact angle was not given by Kazakova, it is expected that contaminated surface has a smaller contact angle compared to clean surface based on the fact that the contamination of the surface improves wettability of the surface [20]. The model predictions well represent the trends of CHF dependency on system pressure except for high pressure above 10 MPa. At high pressure, the model generally tends to overestimate the data. This overestimation seems to result from the inaccuracy of the bubble departure diameter correlation caused by the lack of available experimental data at high pressure [22].

4.2. Comparison with CHF data in subcooled forced convection boiling

The present model is compared with the CHF data from KAIST CHF database [27]. The KAIST database consists of the CHF data for water flow in vertical round tubes, annuli, rectangular channels and rod bundles. For the vertical round tubes, over 14,000 data are compiled from world wide sources. Among them, 2438 subcooled boiling CHF data for upward flow of water in uniformly-heated round tubes are selected for the present study. The selected data set cover the following operating ranges: $0.1 \leqslant P \leqslant 14.0$ MPa, $0.00033 \leqslant D \leqslant 0.0375$ m; $0.002 \leqslant \geqslant L \leqslant 2$ m; $660 \leqslant G \leqslant 90000$ kg/m^2 s; $70 \leqslant \Delta h_i \leqslant 1456$ kJ/kg. Fig. 2 shows a comparison between experimental and calculated CHFs at inlet conditions with contact angle 50°. 1492 data points out of 2438 (61.2%) are calculated. 946 points are not calculated because active site density decreases or wall temperature approaches critical temperature as noted previously. About 80% of calculated data points are predicted within ±50%, with a r.m.s. of 41.3%. As the contact angle increases, average predicted to measured CHF ratios (CHFR) decrease and calculated data points increase. For example, the calculation shows calculated data points of 1237 and 1731, and r.m.s. errors of 41.6 and 38.9%, for contact angles 40 and 60°, respectively. This is due to the fact that the present model largely depends on $\tilde{N}A$. The bubble

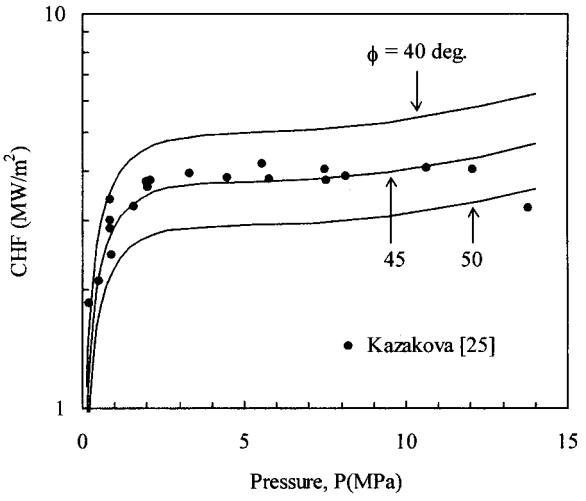

Fig. 1. Comparison of predictions with data for pool boiling.

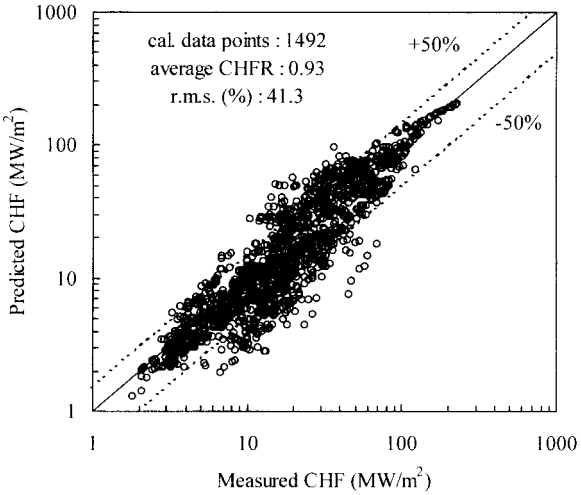

Fig. 2. Experimental vs calculated CHF with contact angle 50°.

Table 2
The capability of the present model compared with existing correlations

Reference	Calculated points	CHFR	r.m.s. error (%)	Cumulative data distribution within error intervals				
				± 10%	± 20%	± 30%	± 40%	± 50%
Present model	1492	0.93	41.3	20.5	38.5	55.8	69.0	79.8
Bowring [28]	1184	0.81	32.1	45.9	59.0	65.3	68.8	77.4
Katto and Ohno [29]	2174	1.24	39.0	25.1	48.5	65.6	75.9	81.6
Katto [15]	698	1.03	17.4	55.4	76.2	93.0	96.8	97.7

diameter increases as the contact angle increases in Eq. (7). And larger bubble diameter results in an increase in $\tilde{N}A$. As a result, premature CHF takes place. When ϕ approaches to zero, the CHF predicted by the present model approaches to infinite value contrary to experimental observations because the bubble departure diameter predicted by Eq. (7) approaches to zero. This is due to the limited applicable range of ϕ in the bubble departure diameter of Fritz. Prediction accuracy for contact angle 50° is compared with well-known CHF correlations and a CHF model in Table 2: Bowring [28] and Katto and Ohno [29] correlations and Katto model [15]. The comparison is limited to the data within the applicable range of each correlation or model. Fig. 3 show the ratio of the calculated to measured CHF for pressure, mass flux, tube diameter and length, in order to check possible systematic effects of the model on CHF prediction. No systematic effect of the pressure on CHF prediction is observed, while the slight underprediction of the CHF can be observed for mass flux lower than 3000 kg/m^2 s, for a tube diameter lower than 0.002 m, and for a length to diameter ratio lower than 10.

4.3. Parametric trends in subcooled forced convection boiling

The parametric trends of subcooled CHF vary according to the thermal–hydraulic conditions and geometric parameters. The parametric trends of CHF for local conditions hypothesis can be summarized as follows [1,30,31]: (1) CHF increases with pressure,

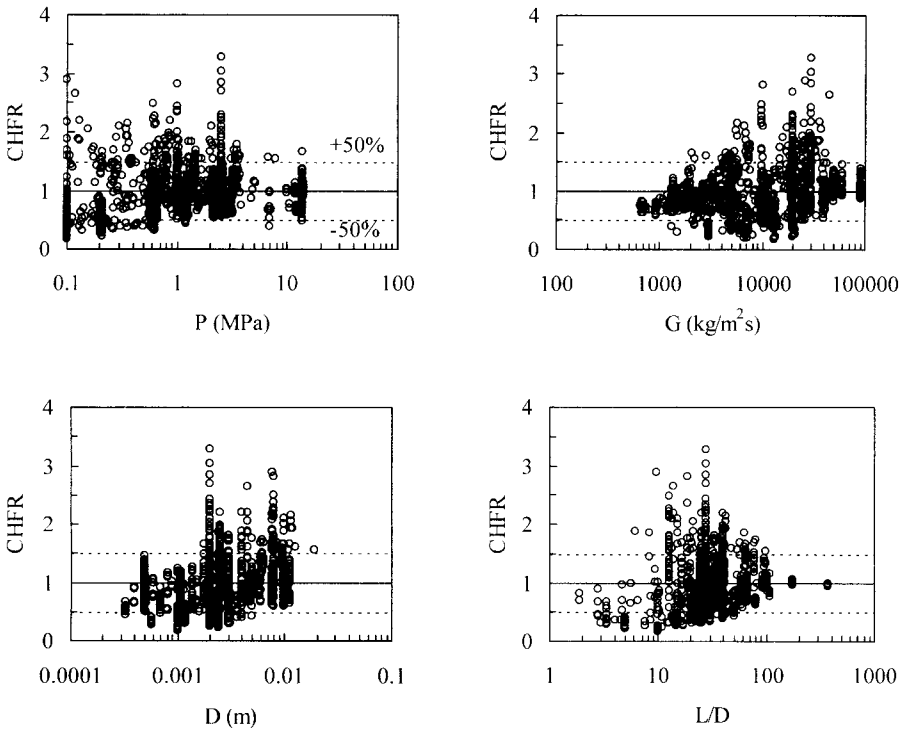

Fig. 3. Ratio of the calculated to experimental vs pressure, mass flux, tube diameter and length.

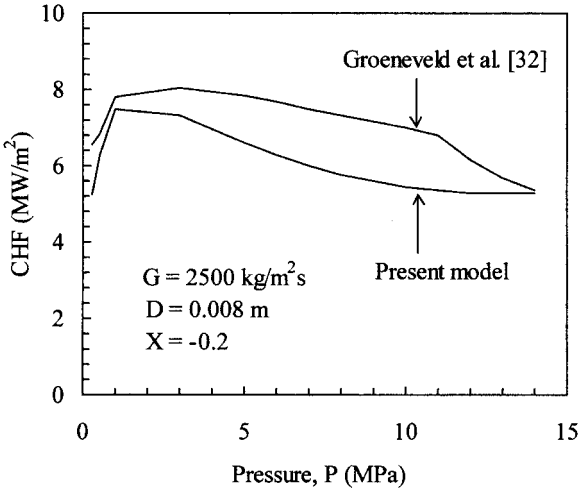

Fig. 4. Pressure effect on CHF.

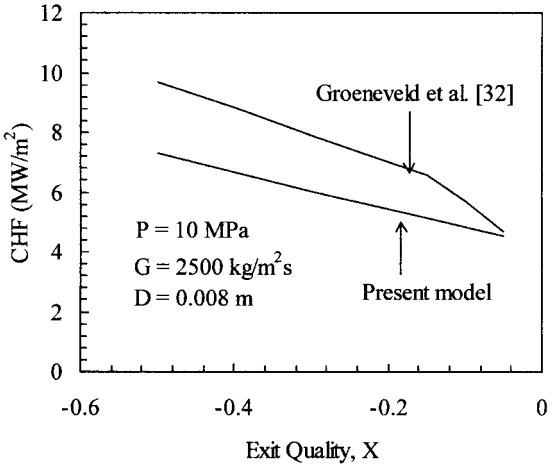

Fig. 6. Exit quality effect on CHF.

passes through a maximum, and then drops off; (2) CHF increases as mass flux increases; (3) CHF decreases as the exit quality increases; and (4) CHF increases as tube diameter decreases.

Figs. 4–7 show the parametric effects on CHF predicted by the present model. The figures also show a comparison with data of 1995 CHF look-up table [32]. Fig. 4 shows that the present model provides the similar trend of CHF vs pressure over a pressure range of interest in the present study. Figs. 5 and 6 show CHF plotted against mass flux and exit quality, respectively. The CHF increases with mass flux and decreases with exit quality. On the contrary to the general observations on the tube diameter effect, the CHF increases, although the degrees of the dependency on tube diameter are different from system pressures, as the tube diameter increase as shown in Fig. 7. There are two reasons for an increase in CHF as diameter increases in the present study. Firstly, the suppression factor used in this study is dependent on Reynolds number only. The suppression factor decreases because Reynolds number increases as the tube diameter increases. Thus, the active site density in Eq. (4) decreases and the CHF increases. However, the assumption made in the suppression factor proposed by Chen [24], which was developed under saturation boiling condition, may not hold any longer for subcooled boiling. As observed by Treshchev [33], the suppression of active nucleation site under subcooled boiling conditions is more sensitive to the degree of liquid subcooling than the flow velocity. Secondly, the effects of tube diameter on bubble diameter are not considered in Eq. (7). As noted by Bergles [34] and Nariai and Inasaka [35], it is expected that as tube diameter decreases, the diameter of bubble becomes

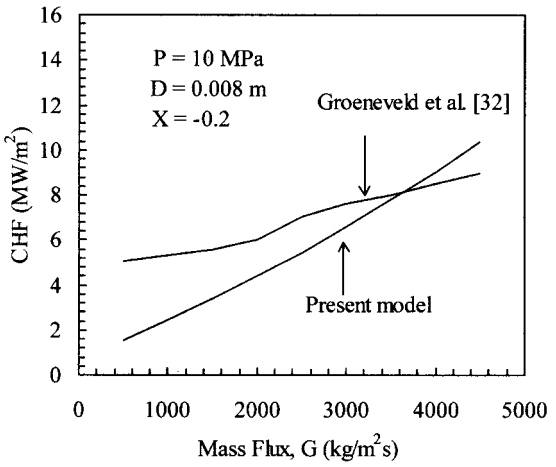

Fig. 5. Mass flux effect on CHF

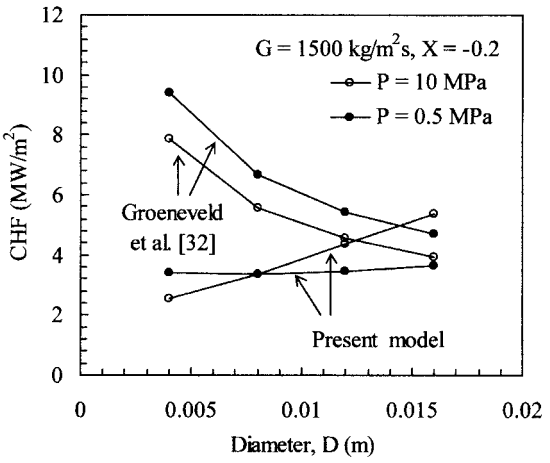

Fig. 7. Diameter effect on CHF.

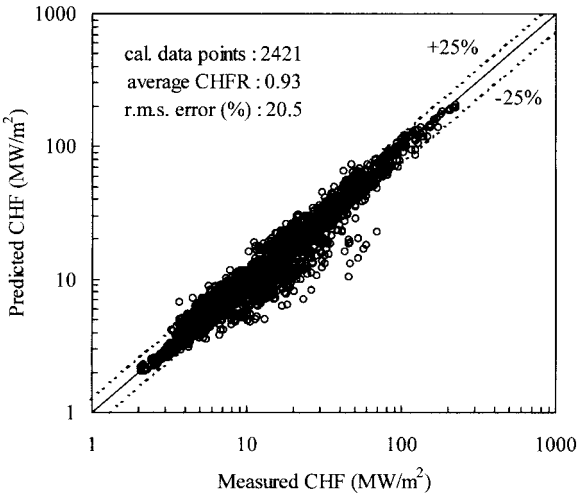

Fig. 8. Experimental vs calculated CHF with a modified suppression factor.

smaller due to the intense condensation effect by subcooled liquid in the core region. Unfortunately, well-established quantitative information is limited. Further works for the effects of tube diameter on bubble diameter and the suppression of nucleation in subcooled boiling are required.

4.4. Modification of suppression factor

As mentioned in the previous section, the suppression of active site density may depend on the degree of liquid subcooling as well as the flow velocity in subcooled forced convection boiling. At the present time none of quantitative information on this is known. To investigate the possibility of the improvement of the predictive capability of the present model by the modification of suppression factor, it is postulated that the suppression factor can be expressed as a function of thermodynamic equilibrium quality X as follows:

$$S = 0.4 + X/1.2 \quad \text{for} \quad X > -0.3, \tag{20}$$

and

$$S = 0.15 \quad \text{for} \quad X \leqslant -0.3 \tag{21}$$

As we know, the thermodynamic equilibrium quality depends on thermal hydraulic conditions and geometric parameters. Fig. 8 shows the comparison between the data and the predictions using the modified suppression factor. This figure shows very good agreement with experimental data. 2421 points out of 2438 (99.3%) are calculated. 36.0, 71.7, and 82.3% of predictions lie within ± 10, $\pm 20\%$, and $\pm 25\%$, respectively. And a global r.m.s. error is 20.5%. The CHF prediction by a modification of suppression factor produces better results than that by the suppression factor proposed by Chen [24]. Therefore, the predictive capability of the present model can be improved with further investigation on the suppression factor in subcooled flow boiling.

5. Summary and conclusion

1. A study has been performed to predict CHF in pool boiling and subcooled forced convection boiling using the dry-spot model presented by the authors and existing correlations for heat transfer coefficient, active site density and bubble departure diameter in nucleate boiling.
2. Comparisons of the model predictions with experimental data for pool boiling of water and subcooled upward forced convection boiling of water in vertical, uniformly-heated round tubes have been performed and the parametric trends of CHF have been investigated. Without any tuning factor, 1492 data points out of the CHF data set (2438 data points) covering wide ranges of operating conditions ($0.1 \leqslant P \leqslant 14.0$ MPa, $0.00033 \leqslant D \leqslant 0.0375$ m; $0.002 \leqslant L \leqslant 2$ m; $660 \leqslant G \leqslant 90000$ kg/m^2 s; $70 \leqslant \Delta h_i \leqslant 1456$ kJ/kg) are calculated with a r.m.s. error of 41.3% and about 80% of the calculated data points are predicted within $\pm 50\%$. It is also shown that by a modification of suppression factor in subcooled boiling, the predictive capability of the present model is improved, i.e. 2421 data points (99.3%) are calculated with a r.m.s. error of 20.5% and 82.3% of the calculated data points are predicted within $\pm 25\%$.
3. The results of the present study strongly support the validity of physical feature of the present model on the CHF mechanism in pool boiling and subcooled forced convection boiling.
4. To improve the prediction capability of the present model, further works on active site density, bubble departure diameter and suppression factor in subcooled boiling are needed.

References

[1] J.G. Collier, J.R. Thome, Convective Boiling and Condensation, 3rd ed., Clarendon Press, Oxford, 1994.
[2] S.H. Chang, W-P. Baek, Critical Heat Flux, Cheong-Moon Gak Publishing Corporation, Seoul, 1997.
[3] J. Weisman, The current status oftheoretically based approaches to the prediction of the critical heat flux in flow boiling, Nucl. Tech. 99 (1992) 1–21.
[4] Y. Katto, Critical heat flux, Int. J. Multiphase Flow 20 (1994) 53–90.
[5] P. Bricard, A. Shouyri, Understanding and modeling

DNB in forced convective boiling: a critical review, in: Proceedings of the International Symposium on Two-Phase Flow Modeling and Experimentation, Rome, 1995, pp. 843–851.
[6] S.H. Chang, W-P. Baek, Perspective on critical heat flux research for reactor design and safety, in: The Fifth International Topical Meeting on Nuclear Thermal Hydraulics, Operations and Safety (NUTHOS-5), Beijing, 1997, pp. AA1-1–AA1-8.
[7] L.S. Tong, H.B. Currin, P.S. Laraen, O.G. Smith, Influences of axially nonuniform heat flux on DNB, Chem. Engr. Prog. Symp. Ser. 62 (64) (1965) 35–40.
[8] W.T. Hancox, W.B. Nicoll, On the dependence of the flow-boiling heat transfer crisis on local near-wall conditions. ASME 73-HT-38, 1973.
[9] B.R. Bergelson, Burnout under conditions of subcooled boiling and forced convection, Thermal Engr. 27 (1) (1980) 48–50.
[10] J. Weisman, B.S. Pei, Prediction of critical heat flux in flow boiling at low qualities, Int. J. Heat Mass Transfer 26 (10) (1983) 1463–1477.
[11] S.H. Chang, K.W. Lee, A critical heat flux model based on mass, energy, and momentum balance for upflow boiling at low qualities, Nucl. Engr. Des. 113 (1989) 35–50.
[12] C.H. Lee, I. Mudawar, A mechanistic critical heat flux model for subcooled flow boiling based on local bulk flow conditions, Int. J. Multiphase Flow 14 (6) (1988) 711–728.
[13] Y. Katto, A physical approach to critical heat flux of subcooled flow boiling in round tubes, Int. J. Heat Mass Transfer 33 (4) (1990) 611–620.
[14] G.P. Celata, M. Cumo, A. Mariani, M. Simoncini, G. Zummo, Rationalization of existing mechanistic models for the prediction of water subcooled flow boiling critical heat flux, Int. J. Heat Mass Transfer 37 (Suppl. 1) (1994) 347–360.
[15] Y. Katto, A prediction model of subcooled water flow boiling CHF for pressure in the range 0.1–20 MPa, Int. J. Heat Mass Transfer 35 (5) (1992) 1115–1123.
[16] Y. Haramura, Y. Katto, A new hydrodynamic model of critical heat flux, applicable widely to boiling to both pool and forced convection boiling on submerged bodies in saturated liquid, Int. J. Heat Mass Transfer 26 (3) (1983) 389–399.
[17] S.J. Ha, H.C. No, A dry-spot model of critical heat flux in pool and forced convection boiling, Int. J. Heat Mass Transfer 41 (2) (1998) 303–311.
[18] M.V.H. Del Valle, D.B.R. Kenning, Subcooled flow boiling at high heat flux, Int. J. Heat Mass Transfer 28 (10) (1985) 1907–1920.
[19] S.J. Ha, H.C. No, A dry-spot model for transition boiling heat transfer in pool boiling, Int. J. Heat Mass Transfer 41 (1998) 3771–3779.
[20] V.K. Dhir, Nucleate and transition boiling heat transfer under pool and external flow conditions, in: Proceedings of the Ninth International Heat Transfer Conference, Jerusalem, vol. 1, 1990, pp. 129–155.
[21] G. Kocamustafaogullari, M. Ishii, Interfacial area and nucleation site density in boiling systems, Int. J. Heat Mass Transfer 26 (9) (1983) 1377–1387.
[22] G. Kocamustafaogullari, Pressure dependence of bubble departure diameter for water, Int. Comm. Heat Mass Transfer 10 (1983) 501–509.
[23] C.Y. Han, P. Griffith, The mechanism of heat transfer in nucleate pool boiling—I. Part bubble initiation, growth and departure, Int. J. Heat Mass Transfer 8 (1965) 887–904.
[24] J.C. Chen, Correlation for boiling heat transfer to saturated fluids in convective flow, I & EC Proc. Des. and Dev. 5 (3) (1966) 322–329.
[25] E.A. Kazakova, The effect of pressure on origination of the first crisis with water boiling on a horizontal plate. Gosenergoizdat, 1953.
[26] Y.Y. Hsu, R.W. Graham, Transport Process in Boiling and Two-Phase Systems, Hemisphere, Washington, 1976.
[27] S.H. Chang et al., The KAIST CHF data bank (rev. 3). KAIST-NUSCOL-9601, 1996.
[28] R.W. Bowring, A simple but accurate round tube uniform heat flux, dryout correlation over the pressure range 0.7–17 MN/m^2 (100–2500 psia). AEEW-R789, 1972.
[29] Y. Katto, H. Ohno, An improved version of the generalized correlation of critical heat flux for the forced convection boiling in uniformly heated vertical tubes, Int. J. Heat Mass Transfer 27 (9) (1984) 1641–1648.
[30] G.P. Celata, Recent achievements in the thermal hydraulics of high heat flux components in fusion reactors, Experimental Thermal and Fluid Science 7 (1993) 263–278.
[31] S.K. Moon, W-P. Baek, S.H. Chang, Parametric trends analysis of the critical heat flux based on artificial neutral networks, Nucl. Engr. Des. 163 (1996) 29–49.
[32] D.C. Groneveld, L.K.H. Leung, P.L. Kirillov, V.P. Bobkov, I.P. Smogaler, V.N. Vinogradov, X.C. Huang, E. Royer, The 1995 look-up table for critical heat flux in tubes, Nucl. Engr. Des. 163 (1996) 1–23.
[33] G.G. Treshchev, The number of vapor-formation centers in surface boiling, in: V.M. Borishonskii, I.T. Pallev (Eds.), Convective Heat Transfer in Two-Phase and One-Phase Flows, 1969, pp. 97–105.
[34] A.E. Bergles, Subcooled burnout in tubes of small diameter tubes. ASME Paper 63-WA-182, 1963.
[35] H. Nariai, F. Inasaka, Critical heat flux and flow characteristics of subcooling flow boiling with water in narrow tubes, in: O.C. Jones, I. Michiyoshi (Eds.), Dynamics of Two-phase Flows, 1992, pp. 689–708.